Pharmacologic Targeting of Sphingosine-1-Phosphate Receptor 1 Improves the Renal Microcirculation during Sepsis in the Mouse

Zhen Wang, Clark R. Sims, Naeem K. Patil, Neriman Gokden, and Philip R. Mayeux

Department of Pharmacology and Toxicology (Z.W., C.R.S., N.K.P., P.R.M.) and Department of Pathology (N.G.), University of Arkansas for Medical Sciences, Little Rock, Arkansas

Received August 14, 2014; accepted October 28, 2014

ABSTRACT

Microvascular failure is hallmark of sepsis in humans and is recognized as a strong predictor of mortality. In the mouse subjected to cecal ligation and puncture (CLP) to induce a clinically relevant sepsis, renal microvascular permeability increases and peritubular capillary perfusion declines rapidly in the kidney leading to acute kidney injury (AKI). Sphingosine-1-phosphate (S1P) is a key regulator of microvascular endothelial function. To investigate the role of S1P in the development of microvascular permeability and peritubular capillary hypoperfusion in the kidney during CLP-induced AKI, we used a pharmacologic approach and a clinically relevant delayed dosing paradigm. Evans blue dye was used to measure renal microvascular permeability and intravital video microscopy was used to quantitate renal cortical capillary perfusion. The S1P receptor 1 (S1P1) agonist SEW2871 [5-[4-phenyl-5-(trifluoromethyl)-2-thienyl]-3-[3-(trifluoromethyl)phenyl]-1,2,4-oxadiazole] and S1P2 antagonist JTE-013 [N-(2,6-dichloro-4-pyridinyl)-2-[1,3-dimethyl-4-(1-methylethyl)-1H-pyrazolo[3,4-b]pyridin-6-yl]-hydrazinecarboxamide] were administered at the time of CLP and produced a dose-dependent but partial reduction in renal microvascular permeability at 6 hours after CLP. However, neither agent improved capillary perfusion at 6 hours. With delayed administration at 6 hours after CLP, only SEW2871 reversed microvascular permeability when measured at 18 hours. Importantly, SEW2871 also restored capillary perfusion and improved renal function. These data suggest that S1P1 and S1P2 do not regulate the early decline in renal capillary perfusion. However, later in the course of sepsis, pharmacologic stimulation of S1P1, even when delaying therapy until after injury has occurred, improves capillary and renal function, suggesting this approach should be evaluated as an adjunct therapy during sepsis.

Introduction

Sepsis is a clinical condition resulting from a severe inflammatory response elicited by a systemic microbial infection (Lee and Slutsky, 2010). It is the eighth leading cause of death in the elderly and the major cause of death in critically ill patients (Angus et al., 2001; Hotchkiss and Karl, 2003). The development of acute kidney injury (AKI) is common in the septic patient and more than doubles the mortality rate to near 70% (Heemskerk et al., 2009). Unfortunately, the foundation of treatment of sepsis remains essentially nonspecific supportive care (Lee and Slutsky, 2010). Moreover, treatment is generally begun only after the onset of symptoms of the systemic inflammatory response syndrome, a time when kidney injury

has likely already been initiated (Zarjou and Agarwal, 2011). Thus, it is critically important to identify new therapeutic targets that could be effective even when therapy is initiated only after diagnosis.

Microvascular dysfunction is a hallmark of sepsis in humans and is newly recognized as a strong predictor of death in patients with severe sepsis (Spanos et al., 2010; De Backer et al., 2013, 2014). In rodent models of sepsis, the renal microcirculation is compromised very early during the development of sepsis-induced AKI (Yasuda et al., 2006; Wu et al., 2007a,b; Wu and Mayeux, 2007; Seely et al., 2011; Wang et al., 2012). These defects include an increase in renal microvascular permeability, a reduction in peritubular capillary perfusion, and regional hypoxia. The mechanisms responsible for renal microcirculatory failure are not fully understood, but an increase in renal microvascular permeability, which precedes the fall in renal capillary perfusion, may contribute to development of decreased flow and vascular congestion (Wu et al., 2007a; Wang et al., 2012). Endothelial cells are a site of injury during systemic inflammation, and disruption of endothelial cell-cell contact is considered an important mechanism for the enhanced

ABBREVIATIONS: AKI, acute kidney injury; BUN, blood urea nitrogen; CLP, cecal ligation and puncture; DMF, dimethylformamide; EBD, Evans blue dye; IVVM, intravital video microscopy; JTE-013, N-(2,6-dichloro-4-pyridinyl)-2-[1,3-dimethyl-4-(1-methylethyl)-1H-pyrazolo[3,4-b]pyridin-6-yl]-hydrazinecarboxamide; MAP, mean arterial pressure; SEW2871, 5-[4-phenyl-5-(trifluoromethyl)-2-thienyl]-3-[3-(trifluoromethyl)phenyl]-1,2,4-oxadiazole; S1P, sphingosine-1-phosphate.

microvascular permeability that occurs during sepsis (Lee and Slutsky, 2010).

Sphingosine-1-phosphate (S1P), a bioactive lysophospholipid generated from intracellular ceramide, has emerged as a key regulator of endothelial stability, vascular permeability, and microvascular function (Lee et al., 1999; Wang and Dudek, 2009; Zeng et al., 2014). S1P acts primarily through five unique G protein–coupled receptors expressed in distinct combinations in different cell types. For example, S1P receptor 1 (S1P1) is coupled to G_i, and in the endothelial cell, S1P1 agonists enhance the permeability barrier through the activation of Rac GTPase, leading to assembly of adheren junctions, cytoskeletal reorganization, and focal adhesion formation (Wang and Dudek, 2009). In contrast, stimulation of S1P receptor 2 (S1P2) in endothelial cells, which couple to G_i, G_q, and $G_{12/13}$, results in Rho-ROCK (RhoA-associated kinase) and PTEN (phosphatase and tensin homologue) dependent disruption of adherens junctions and an increase in paracellular permeability (Sanchez et al., 2007). Hence, the balance between the activation and/or regulation of S1P1 and S1P2 may control the regulation of vascular permeability by S1P in the microcirculation.

In addition to endothelial cells, S1P1 and S1P2 are expressed by the renal epithelium; however, expression can vary in different regions of the kidney, and their function has not been fully characterized (Zhu et al., 2011; Park et al., 2012). Agonists to S1P1 and antagonists to S1P2 protect against renal ischemia/reperfusion injury (Awad et al., 2006; Park et al., 2012). Interestingly, selective deletion of endothelial S1P1 (Ham et al., 2014) or proximal tubule S1P1 (Bajwa et al., 2010) exacerbates renal ischemia/reperfusion injury, suggesting a cross-talk between the renal microvasculature and tubular epithelium during renal ischemia, which has also been suggested to occur during sepsis (Mayeux and Macmillan-Crow, 2012). Recent studies in the kidney also suggest that S1P could be a physiologic regulator of preglomerular vascular tone (Guan et al., 2014).

To evaluate the role of S1P1 and S1P2 in septic AKI, preclinical studies in mice were performed with SEW2871 [5-[4-phenyl-5-(trifluoromethyl)-2-thienyl]-3-[3-(trifluoromethyl)phenyl]-1,2,4-oxadiazole], an S1P1 agonist (Sanna et al., 2004), and JTE-013 [N-(2,6-dichloro-4-pyridinyl)-2-[1,3-dimethyl-4-(1-methylethyl)-1H-pyrazolo[3,4-b]pyridin-6-yl]-hydrazinecarboxamide], an S1P2 antagonist (Osada et al., 2002), to examine their effects on renal microvascular permeability and capillary perfusion. Because therapy in the septic patient is usually begun only after the onset of symptoms, these agents were evaluated using a clinically relevant delayed dosing paradigm.

Materials and Methods

Fluorescein isothiocyanate-dextran 500,000-Da conjugate, fatty acid, and globulin-free bovine serum albumin, dimethylformamide (DMF), formamide, and Evans blue dye (EBD) were purchased from Sigma-Aldrich (St. Louis, MO). SEW2871 and JTE-013 were purchased from Cayman Chemical Company (Ann Arbor, MI).

Cecal Ligation and Puncture Model of Sepsis. Cecal ligation and puncture (CLP) was performed on male C57/BL6 mice (Harlan, Indianapolis, IN) aged 38–40 weeks as described previously elsewhere (Miyaji et al., 2003; Yasuda et al., 2006; Wu et al., 2007a). While the mice were under isoflurane anesthesia, 1.5 cm of the cecal tip was ligated using a 4-0 silk suture and punctured through and through with a 21-gauge needle. Approximately a 1-mm column of fecal material was expressed through each opening. In sham-operated mice (sham), the cecum was isolated but neither ligated nor punctured. After surgery, all

mice received 1 ml of prewarmed saline and were placed in individual cages on a heating pad. Mice studied at time points longer than 6 hours were given imipenem/cilastatin (14 mg/kg) and 1.5 ml of normal saline (40 ml/kg) by subcutaneous injection at 6 hours. All animals were housed and handled in accordance to the National Institutes of Health Guide for the Care of Laboratory Animals with approval from an internal animal care and use committee.

Administration of SEW2871 and JTE-013. Fresh solutions of SEW2871 and JTE-013 were prepared in DMF, kept in the dark, and further diluted to the desired concentrations in 3% fatty acid and globulin-free bovine serum albumin in phosphate-buffered saline (DMF vehicle) just before use. SEW2871 was evaluated at doses of 1, 3, 10, 30 mg/kg. JTE-013 was evaluated at doses of 0.1, 1, 10 mg/kg. Mice were treated with SEW2871, JTE-013, or DMF vehicle in a volume of 2 μl/g body weight by intraperitoneal injection.

Intravital Video Microscopy. Intravital video microscopy (IVVM) was performed as described previously elsewhere (Wang et al., 2012; Holthoff et al., 2013). Briefly, after anesthesia with isoflurane, fluorescein isothiocyanate-labeled dextran (2 μmol/kg in 3 ml/kg normal saline) was administered via the penile vein to visualize the capillary vascular space. After 10 minutes, the left kidney was exposed by a flank incision and positioned on a glass stage above an inverted Zeiss Axiovert 200M fluorescent microscope equipped with an Axiocam HSm camera (Zeiss, Germany). Videos of 10 seconds (approximately 30 frames/seconds) at 200× magnification were acquired from five randomly selected, nonoverlapping fields of view. Body temperature was maintained at 35–37°C with a warming lamp.

Assessment of Renal Microcirculation. Approximately 150 capillaries were analyzed from the kidney of each animal. Capillaries were randomly selected from each of the videos collected during IVVM and categorized as "continuous" where red blood cell movement was uninterrupted; "intermittent" where red blood cell movement stopped or reversed; or "no flow" where no red blood cell movement was observed. Data were expressed as the percentage of vessels in each of the three categories.

Assessment of Renal Microvascular Permeability Using Evans Blue Dye. Renal microvascular permeability was assessed as described by Yasuda et al. (2006) with slight modifications (Wang et al., 2012; Holthoff et al., 2013). At 30 minutes before killing, EBD (1% in 0.9% saline) was injected at 2 ml/kg via the tail vein. At killing, mice were perfused with 30 ml of phosphate-buffered saline through the left ventricle until all blood was eliminated. The right kidney was weighed, homogenized in 1 ml formamide, and then incubated at 55°C for 18 hours. The homogenate was then centrifuged at 12,000g for 30 minutes, and the supernatant was collected. EBD was quantified in the supernatant by measuring absorbance at 620 nm and correcting for turbidity at 740 nm, as described by Moitra et al. (2007). Concentrations of EBD were determined from a standard curve and expressed as micrograms per gram kidney wet weight (right kidney).

Measurement of Mean Arterial Pressure in Conscious Mice. Mean arterial pressure was monitored continuously in conscious mice using biotelemetry as described previously elsewhere (Wang et al., 2012; Holthoff et al., 2013). Transmitters (Data Sciences International, Minneapolis, MN) were implanted into the carotid artery under isoflurane anesthesia, and the mice were allowed to recover for 5 days. Mice were reanesthetized with isoflurane, and sepsis was induced by CLP. Mean arterial pressure was recorded for 10 seconds every 5 minutes.

Serum Blood Urea Nitrogen and Creatinine. Blood urea nitrogen (BUN) and creatinine concentrations in serum were measured using the QuantiChrom Urea Assay kit and Creatinine Assay kit, respectively (BioAssay Systems, Hayward, CA). Data were expressed as milligrams per deciliter of serum.

Histologic Analysis of Renal Morphology. Kidney sections were stained for glycoproteins using the periodic acid–Schiff method and scored in a blinded, semiquantitative manner. For each mouse, at least 10 high-power (400× magnification) fields were examined. The percentage of tubules that displayed cellular necrosis, loss of brush
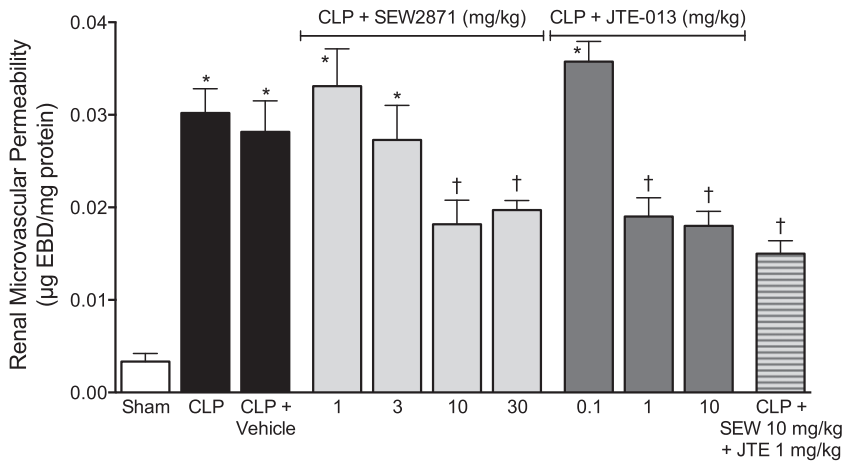
Fig. 1. Effects of SEW2871 and JTE-013 on renal microvascular permeability at 6 hours after CLP. At the time of CLP, mice received vehicle ($n = 9$), various doses of SEW2871 ($n = 6–11$) or JTE-013 ($n = 4–6$), or the combination of SEW2871 and JTE-013 ($n = 6$). At 6 hours, Evans blue dye was used to measure microvascular permeability. There was a significant increase in renal microvascular permeability in the CLP ($n = 5$) and CLP + vehicle groups compared with the sham group ($n = 6$). Both SEW2871 and JTE-013 produced partial but significant dose-dependent decreases in microvascular permeability. The combination of SEW2871 and JTE-013 produced no additional decrease. Data are mean ± S.E.M.; *$P < 0.05$ compared with the sham group; †$P < 0.05$ compare with the CLP group.

border, cast formation, vacuolization, and tubule dilation were scored as follows: 0 = none, 1 ≤ 10%, 2 = 11–25%, 3 = 26–45%, 4 = 46–75%, and 5 ≥ 76%.

Statistical Analysis. Data, presented as mean ± S.E.M., were analyzed using Prism 5.0 (GraphPad Software, San Diego, CA). Data with three or more groups were analyzed using a one-way analysis of variance followed by the Bonferroni or Newman-Keuls post hoc tests with the exception of the renal tubular injury scores, which were analyzed using the nonparametric Kruskal-Wallis test followed by the Dunn multiple-comparisons test. $P < 0.05$ were considered statistically significant.

Results

Dose-Response Effects of SEW2871 and JTE-013 on Renal Microvascular Permeability at 6 Hours after CLP. Increased microvascular permeability is one key component of vascular dysfunction associated with sepsis-induced organ injury (Kumar et al., 2009). In the mouse, an increase in vascular permeability in the kidney is one of the earliest events after CLP (Wang et al., 2012). The roles of S1P1 and S1P2 were evaluated using the S1P1 agonist SEW2871 at doses of 1, 3, 10, and 30 mg/kg and the S1P2 antagonist JTE-013 at doses of and 0.1, 1.0, and 10 mg/kg. The vehicle or each agent was administered at the time of CLP by intraperitoneal injection.

In the CLP and CLP + vehicle groups, microvascular permeability was significantly increased at 6 hours compared with the sham group (Fig. 1). There was no difference between the CLP alone and CLP + vehicle groups, indicating that the vehicle itself did not alter permeability.

SEW2871 at doses of 10 and 30 mg/kg significantly, but incompletely, decreased microvascular permeability. JTE-013 at doses of 1 and 10 mg/kg also significantly, but incompletely, decreased microvascular permeability. To determine whether a combination of these agents could further reduce permeability, mice were administered SEW2871 at 10 mg/kg and JTE-013 at 1 mg/kg, the lowest doses of each that significantly reduced permeability alone. The combination did not reduce permeability more than either agent alone.

Effects of SEW2871 and JTE-013 on Renal Peritubular Capillary Perfusion at 6 Hours after CLP. Using IVVM, we categorized the cortical distribution of peritubular capillary perfusion as continuous, intermittent, or no flow. At 6 hours after CLP, the percentage of capillaries with continuous perfusion was significantly reduced, and the percentage of

capillaries with intermittent and no perfusion was significantly increased compared with sham control (Fig. 2). The most efficacious doses of SEW2871 (10 mg/kg) and JTE-013 (1 mg/kg) to reduce permeability were evaluated for their effects on the renal capillary perfusion at 6 hours. Vehicle or each agent was administered at the time of CLP surgery. Treatment with SEW2871 or JTE-013 (Fig. 2) at doses that reduced renal microvascular permeability had no effect on the renal cortical peritubular capillary perfusion at 6 hours after CLP compared with vehicle alone.

Delayed Treatment with SEW2871 or JTE-013 on Renal Peritubular Microvascular Permeability at 18 Hours after CLP. Therapy in the septic patient is most often begun only after the onset of symptoms (Russell, 2006). To evaluate the clinically relevant therapeutic potential of SEW2871 and JTE-013 we used a delayed dosing paradigm. These agents were administered at 6 hours after CLP because this is the time of greatest increase in renal microvascular permeability and greatest decline in renal capillary perfusion (Wang et al., 2012). At 18 hours after CLP, microvascular permeability remained elevated compared with the sham group. Similar to what was observed at 6 hours after CLP, delayed administration of vehicle also did not affect CLP-induced permeability at
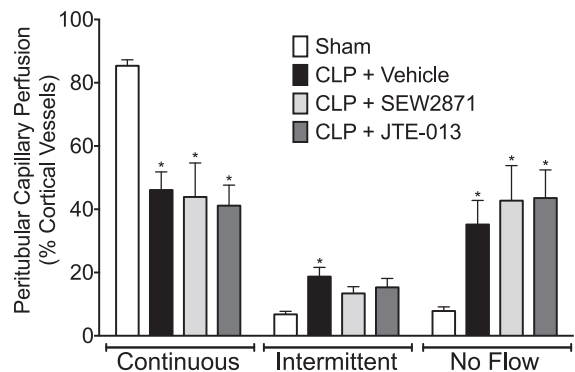

Fig. 2. Effect of SEW2871 and JTE-013 on renal peritubular capillary perfusion at 6 hours after CLP. At 6 hours after CLP, there were significant decreases in the percentage of cortical peritubular capillaries with continuous flow and increases in the percentage with intermittent and no flow. Neither SEW2871 (10 mg/kg) nor JTE-013 (1 mg/kg), administered at the time of CLP, altered the distribution of capillaries with continuous or no flow. Data are mean ± S.E.M.; *$P < 0.05$ compared with the sham group; $n = 7$ in sham, $n = 9$ in CLP + vehicle, $n = 5$ in CLP + SEW2871, and $n = 5$ in CLP + JTE-013.

18 hours; therefore, the CLP and CLP + vehicle groups were combined in Fig. 3. We chose to test the lowest most efficacious doses of SEW2871 (10 mg/kg) and JTE-013 (1 mg/kg), determined in Fig. 1, using this delayed dosing paradigm. Delaying treatment until 6 hours after CLP with SEW2871 reversed renal microvascular permeability to levels not different from the sham group (Fig. 3). In contrast, delayed treatment with JTE-013 at 1 mg/kg did not reverse renal microvascular permeability. To help confirm the absence of efficacy, we also tested JTE-013 at 10 mg/kg. Even this higher dose did not reduce microvascular permeability.

Effect of Delayed Therapy with SEW2871 on Renal Peritubular Capillary Perfusion. CLP in the mouse produces a sustained decrease in peritubular capillary perfusion (Wang et al., 2012). Because SEW2871 reversed microvascular permeability even with delayed therapy, it was evaluated further for possible effects on the decreases in peritubular capillary perfusion at 18 hours. Even when administered at 6 hours after CLP, SEW2871 (10 mg/kg) reversed the decrease in peritubular capillary perfusion (Fig. 4).

Effect of Delayed Therapy with SEW2871 on Mean Arterial Pressure. Our model of sepsis is one of severe sepsis associated with hypotension (Holthoff et al., 2012, 2013; Wang et al., 2012). Because agents that increase mean arterial pressure (MAP) could increase peritubular capillary perfusion without exerting any direct action on renal capillaries, the effects of vehicle and SEW2871 on MAP were evaluated in conscious mice by biotelemetry (Fig. 5). CLP produced a rapid fall in MAP that persisted through 18 hours. Neither vehicle nor SEW2871 (10 mg/kg) administered at 6 hours after CLP significantly altered MAP when compared with mice subjected to CLP alone.

Effect of Delayed Therapy with SEW2871 on Renal Function and Morphology. At 18 hours after CLP, two clinical markers of renal function, serum BUN and creatinine, indicated a decline in renal function. Treatment with SEW2871 (10 mg/kg) at 6 hours after CLP, a time when glomerular filtration is already decreased and serum BUN is already elevated (Wang et al., 2012; Leelahavanichkul et al., 2014; Patil et al., 2014),
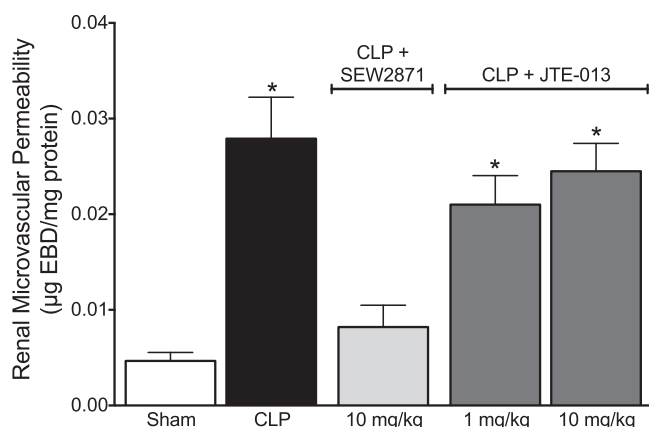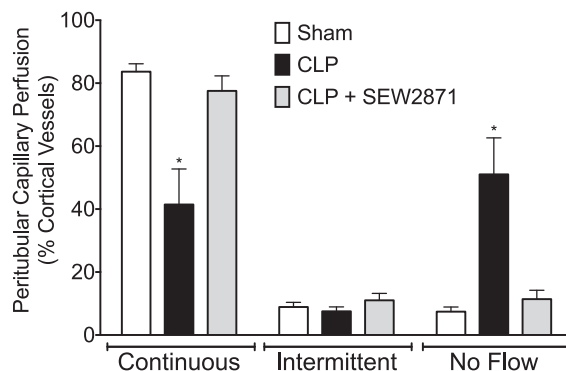
Fig. 4. Effects of delayed treatment with SEW2871 on peritubular capillary perfusion at 18 hours after CLP. SEW2871 (10 mg/kg) administered 6 hours after CLP restored the distribution of peritubular capillary perfusion to the levels in the sham group. Data are mean ± S.E.M.; *P < 0.05 compared with sham; n = 6 in sham, n = 8 in CLP, and n = 8 in CLP + SEW2871.

significantly reduced the serum levels of BUN and prevented the increase in serum creatinine (Fig. 6, A and B). However, measurements of serum creatinine using the picrate colorimetric method must be interpreted with caution (Meyer et al., 1985; Yuen et al., 2004). At 18 hours after CLP, the changes in kidney morphology were evident but relatively mild and included some loss of brush border, tubular degeneration, and vacuolization. SEW2871 also improved the kidney morphology injury score (Fig. 6C). Taken together, these findings along with improved capillary perfusion suggest that even delayed treatment with SEW2871 improved but did not fully restore renal function.

Discussion

Within the first few hours after CLP in the mouse, cytokines are elevated (Miyaji et al., 2003; Wang et al., 2011), renal microvascular permeability increases (Wang et al., 2012), and the fall in peritubular capillary perfusion parallels the fall in MAP (Holthoff et al., 2012; Wang et al., 2012). As sepsis progresses, renal epithelial oxidant generation and tubular injury appear to extend microvascular injury and impede recovery (Wang et al., 2011; Patil et al., 2014).

In this study we used a pharmacologic approach to examine the relationships between renal vascular permeability, peritubular capillary perfusion, and renal function by targeting S1P receptors in CLP-induced sepsis, a clinically relevant model of sepsis-induced AKI. An important finding from our previous study was the demonstration of early renal capillary dysfunction that included the rapid increase in microvascular permeability followed by a decrease in renal capillary perfusion (Wang et al., 2012). Renal capillary hypoperfusion during sepsis can lead to regional hypoxia (Yasuda et al., 2006) and an increase in tubular epithelial redox stress (Wu and Mayeux, 2007). Increased microvascular permeability could also increase leukocytes extravasation and extracellular edema (Bajwa et al., 2010), which could contribute to tubular epithelial damage. Because both decreased perfusion and increased permeability of the renal microvasculature can promote renal tubular cell injury, we reasoned that targeting microvascular dysfunction might protect the tubular epithelium and overall renal function.

The doses of SEW2871 and JTE-013 tested were based on studies evaluating these agents in renal ischemic injury (Awad et al., 2006; Park et al., 2012). With pretreatment, each

Fig. 3. Effect of delayed treatment with SEW2871 and JTE-013 on renal microvascular permeability at 18 hours after CLP. At 18 hours after CLP, microvascular permeability was significantly increased. Administration of SEW2871 (10 mg/kg) at 6 hours after CLP, a time when microvascular permeability was already increased (Fig. 1), resulted in a decrease in microvascular permeability when measured at 18 hours. In contrast, JTE-013 at 1 or 10 mg/kg administered at 6 hours after CLP had no effect on microvascular permeability at 18 hours. Data are mean ± S.E.M.; *P < 0.05 compared with sham; n = 6 in sham, n = 8 in CLP, n = 5 in CLP + SEW2871, and n = 4–5 in CLP + JTE-013 groups.
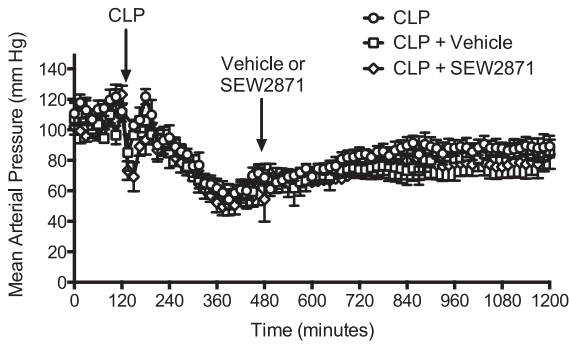
Fig. 5. Effects of delayed treatment with SEW2871 on MAP after CLP. Depicted is the time course of MAP measured in three groups of conscious mice using biotelemetry. All mice received CLP at the time indicated by the arrow. At 6 hours, the CLP + vehicle group ($n = 3$) received vehicle, and the CLP + SEW2871 group ($n = 4$) received SEW2871 at a dose of 10 mg/kg. Neither vehicle nor SEW2871 had any significant effect on MAP when compared with the CLP group ($n = 5$). Data are mean ± S.E.M.

agent produced a dose-dependent decrease in microvascular permeability at 6 hours after CLP; however, the protection against leakage was incomplete, and the combination of the two agents at the lowest most efficacious dose of each provided no further protection. Sepsis-induced endothelial injury is orchestrated through a complex series of interrelated pathways (Aird, 2003; Lee and Liles, 2011). Nevertheless, stimulating S1P1 with SEW2871 or inhibiting S1P2 with JTE-031 did reduce permeability when these agents were administered at the time of CLP. Next, using the lowest most efficacious doses of SEW2871 and JTE-031 determined in the permeability dose-finding study, we evaluated their effects on capillary perfusion within the first 6 hours. Interestingly, neither agent protected against the initial decline in capillary perfusion. This is a significant finding because it dissociates the early fall in capillary perfusion from microvascular permeability and supports the notion that the initial fall in renal microvascular perfusion is more directly dependent on the rapid fall in renal blood flow that occurs in this model of severe sepsis (Wang et al., 2012).

To examine whether these agents may have therapeutic potential to target microvascular injury that is likely to be present by the time of diagnosis in the septic patient, we treated animals at 6 hours after CLP, a time when microvascular permeability was already increased and capillary perfusion was already decreased. Under these conditions, SEW2871 was actually able to reverse microvascular leakage. In contrast, JTE-013, tested at two doses, was ineffective. Taken together, these findings suggest that stimulation of S1P1 is preventative as well as reparative, whereas antagonism of S1P2 appears to only be preventative. This is consistent with the report that pretreatment with JTE-013 in a murine lipopolysaccharide model of sepsis reduced inflammatory cytokines and endothelial activation (Zhang et al., 2013). However, our studies using a delayed dosing paradigm begun after the initial cytokine release (Miyaji et al., 2003; Wang et al., 2011) to more appropriately mimic the clinical setting suggest that targeting S1P2, at least with JTE-013, may not be as effective as targeting S1P1.

Further evidence of the therapeutic potential of targeting S1P1 comes from the findings that even delayed administration of SEW2871 dramatically improved capillary perfusion. The ability of SEW2871 to restore renal capillary perfusion without increasing MAP suggests a direct effect on the renal
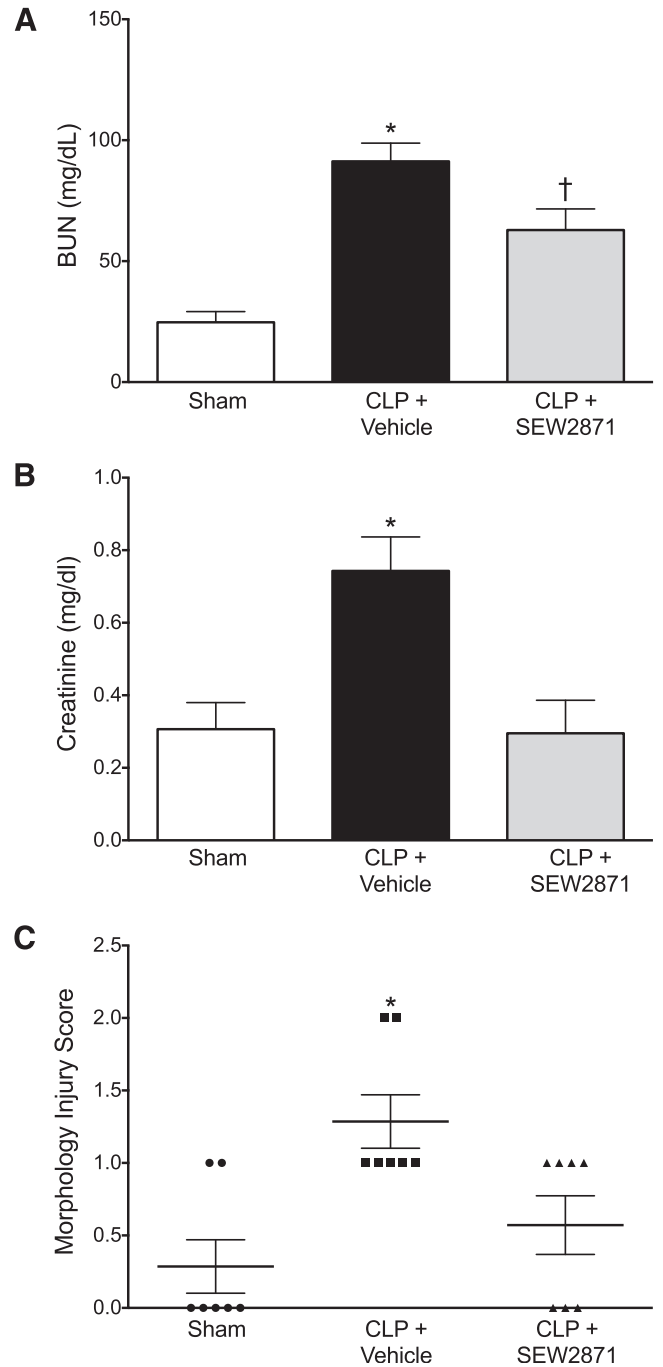

Fig. 6. Effects of delayed treatment with SEW2871 on renal function and morphology at 18 hours after CLP. CLP caused an increase in serum BUN and creatinine concentrations as well as an increase in the kidney morphology score. Administration of SEW2871 (10 mg/kg) at 6 hours after CLP decreased serum BUN (A) and creatinine (B) levels at 18 hours. Data are mean ± S.E.M.; *$P < 0.05$ compared with the sham group; †$P < 0.05$ compared with the CLP + vehicle and sham groups; $n = 8$ in sham; $n = 11$ in CLP + vehicle; $n = 6$ in CLP + SEW2871. SEW2871 decreased the kidney morphology score (C). Individual scores are shown along with mean ± S.E.M.; *$P < 0.05$; $n = 7$ animals per group.

microcirculation. However, S1P1 is also expressed in renal tubules (Zhu et al., 2011), and SEW2871 did improve morphology, suggesting that SEW2871 could act at multiple sites within the kidney to improve but not completely restore overall renal function during sepsis, as has been observed in delayed therapy with other agents (Miyaji et al., 2003; Yasuda et al., 2006; Wang

et al., 2012; Holthoff et al., 2013). The protective effects of SEW2871 in the sepsis model are consistent with the findings in renal ischemia/reperfusion injury where selective deletion of endothelial S1P1 (Ham et al., 2014) or proximal tubule S1P1 (Bajwa et al., 2010) both exacerbate renal injury. Additional studies are needed to establish the mechanisms of action of S1P1 agonists and mode of signaling cross-talk in the kidney, which could promote recovery of the microvasculature and the tubular epithelium.

These initial preclinical studies suggest that targeting S1P1 with SEW2871, even after the initiation of injury can improve renal function. These findings support the growing realization that repair of the microcirculation may actually be more important than simply raising MAP to protect organ function (De Backer et al., 2013; Asfar et al., 2014). If confirmed as a class, the addition of S1P1 agonists to current supportive therapy might be a new promising strategy to prevent further injury and promote recovery.

Authorship Contributions

Participated in research design: Wang, Mayeux.
Conducted experiments: Wang, Patil, Sims.
Performed data analysis: Wang, Sims, Gokden, Mayeux.
Wrote or contributed to the writing of the manuscript: Wang, Sims, Mayeux.

References

Aird WC (2003) The role of the endothelium in severe sepsis and multiple organ dysfunction syndrome. *Blood* 101:3765–3777.
Angus DC, Linde-Zwirble WT, Lidicker J, Clermont G, Carcillo J, and Pinsky MR (2001) Epidemiology of severe sepsis in the United States: analysis of incidence, outcome, and associated costs of care. *Crit Care Med* 29:1303–1310.
Asfar P, Meziani F, Hamel JF, Grelon F, Megarbane B, Anguel N, Mira JP, Dequin PF, Gergaud S, and Weiss N, et al.; SEPSISPAM Investigators (2014) High versus low blood-pressure target in patients with septic shock. *N Engl J Med* 370: 1583–1593.
Awad AS, Ye H, Huang L, Li L, Foss FW, Jr, Macdonald TL, Lynch KR, and Okusa MD (2006) Selective sphingosine 1-phosphate 1 receptor activation reduces ischemia-reperfusion injury in mouse kidney. *Am J Physiol Renal Physiol* 290:F1516–F1524.
Bajwa A, Jo SK, Ye H, Huang L, Dondeti KR, Rosin DL, Haase VH, Macdonald TL, Lynch KR, and Okusa MD (2010) Activation of sphingosine-1-phosphate 1 receptor in the proximal tubule protects against ischemia-reperfusion injury. *J Am Soc Nephrol* 21:955–965.
De Backer D, Donadello K, Sakr Y, Ospina-Tascon G, Salgado D, Scolletta S, and Vincent JL (2013) Microcirculatory alterations in patients with severe sepsis: impact of time of assessment and relationship with outcome. *Crit Care Med* 41: 791–799.
De Backer D, Orbegozo Cortes D, Donadello K, and Vincent JL (2014) Pathophysiology of microcirculatory dysfunction and the pathogenesis of septic shock. *Virulence* 5:73–79.
Guan Z, Singletary ST, Cook AK, Hobbs JL, Pollock JS, and Inscho EW (2014) Sphingosine-1-phosphate evokes unique segment-specific vasoconstriction of the renal microvasculature. *J Am Soc Nephrol* 25:1774–1785.
Ham A, Kim M, Kim JY, Brown KM, Fruttiger M, D'Agati VD, and Lee HT (2014) Selective deletion of the endothelial sphingosine-1-phosphate 1 receptor exacerbates kidney ischemia-reperfusion injury. *Kidney Int* 85:807–823.
Heemskerk S, Masereeuw R, Russel FG, and Pickkers P (2009) Selective iNOS inhibition for the treatment of sepsis-induced acute kidney injury. *Nat Rev Nephrol* 5:629–640.
Holthoff JH, Wang Z, Patil NK, Gokden N, and Mayeux PR (2013) Rolipram improves renal perfusion and function during sepsis in the mouse. *J Pharmacol Exp Ther* 347:357–364.
Holthoff JH, Wang Z, Seely KA, Gokden N, and Mayeux PR (2012) Resveratrol improves renal microcirculation, protects the tubular epithelium, and prolongs survival in a mouse model of sepsis-induced acute kidney injury. *Kidney Int* 81: 370–378.
Hotchkiss RS and Karl IE (2003) The pathophysiology and treatment of sepsis. *N Engl J Med* 348:138–150.
Kumar P, Shen Q, Pivetti CD, Lee ES, Wu MH, and Yuan SY (2009) Molecular mechanisms of endothelial hyperpermeability: implications in inflammation. *Expert Rev Mol Med* 11:e19.
Lee MJ, Thangada S, Claffey KP, Ancellin N, Liu CH, Kluk M, Volpi M, Sha'afi RI, and Hla T (1999) Vascular endothelial cell adherens junction assembly and morphogenesis induced by sphingosine-1-phosphate. *Cell* 99:301–312.

Lee WL and Liles WC (2011) Endothelial activation, dysfunction and permeability during severe infections. *Curr Opin Hematol* 18:191–196.
Lee WL and Slutsky AS (2010) Sepsis and endothelial permeability. *N Engl J Med* 363:689–691.
Leelahavanichkul A, Souza AC, Street JM, Hsu V, Tsuji T, Doi K, Li L, Hu X, Zhou H, and Kumar P, et al. (2014) Comparison of serum creatinine and serum cystatin C as biomarkers to detect sepsis-induced acute kidney injury and to predict mortality in CD-1 mice. *Am J Physiol Renal Physiol* 307:F939–F948.
Mayeux PR and MacMillan-Crow LA (2012) Pharmacological targets in the renal peritubular microenvironment: implications for therapy for sepsis-induced acute kidney injury. *Pharmacol Ther* 134:139–155.
Meyer MH, Meyer RA, Jr, Gray RW, and Irwin RL (1985) Picric acid methods greatly overestimate serum creatinine in mice: more accurate results with high-performance liquid chromatography. *Anal Biochem* 144:285–290.
Miyaji T, Hu X, Yuen PS, Muramatsu Y, Iyer S, Hewitt SM, and Star RA (2003) Ethyl pyruvate decreases sepsis-induced acute renal failure and multiple organ damage in aged mice. *Kidney Int* 64:1620–1631.
Moitra J, Sammani S, and Garcia JG (2007) Re-evaluation of Evans blue dye as a marker of albumin clearance in murine models of acute lung injury. *Transl Res* 150:253–265.
Osada M, Yatomi Y, Ohmori T, Ikeda H, and Ozaki Y (2002) Enhancement of sphingosine 1-phosphate-induced migration of vascular endothelial cells and smooth muscle cells by an EDG-5 antagonist. *Biochem Biophys Res Commun* 299: 483–487.
Park SW, Kim M, Brown KM, D'Agati VD, and Lee HT (2012) Inhibition of sphingosine 1-phosphate receptor 2 protects against renal ischemia-reperfusion injury. *J Am Soc Nephrol* 23:266–280.
Patil NK, Parajuli N, MacMillan-Crow LA, and Mayeux PR (2014) Inactivation of renal mitochondrial respiratory complexes and manganese superoxide dismutase during sepsis: mitochondria-targeted antioxidant mitigates injury. *Am J Physiol Renal Physiol* 306:F734–F743.
Russell JA (2006) Management of sepsis. *N Engl J Med* 355:1699–1713.
Sanchez T, Skoura A, Wu MT, Casserly B, Harrington EO, and Hla T (2007) Induction of vascular permeability by the sphingosine-1-phosphate receptor-2 (S1P2R) and its downstream effectors ROCK and PTEN. *Arterioscler Thromb Vasc Biol* 27:1312–1318.
Sanna MG, Liao J, Jo E, Alfonso C, Ahn MY, Peterson MS, Webb B, Lefebvre S, Chun J, and Gray N, et al. (2004) Sphingosine 1-phosphate (S1P) receptor subtypes S1P1 and S1P3, respectively, regulate lymphocyte recirculation and heart rate. *J Biol Chem* 279:13839–13848.
Seely KA, Holthoff JH, Burns ST, Wang Z, Thakali KM, Gokden N, Rhee SW, and Mayeux PR (2011) Hemodynamic changes in the kidney in a pediatric rat model of sepsis-induced acute kidney injury. *Am J Physiol Renal Physiol* 301: F209–F217.
Spanos A, Jhanji S, Vivian-Smith A, Harris T, and Pearse RM (2010) Early microvascular changes in sepsis and severe sepsis. *Shock* 33:387–391.
Wang L and Dudek SM (2009) Regulation of vascular permeability by sphingosine 1-phosphate. *Microvasc Res* 77:39–45.
Wang Z, Herzog C, Kaushal GP, Gokden N, and Mayeux PR (2011) Actinonin, a meprin A inhibitor, protects the renal microcirculation during sepsis. *Shock* 35:141–147.
Wang Z, Holthoff JH, Seely KA, Pathak E, Spencer HJ, 3rd, Gokden N, and Mayeux PR (2012) Development of oxidative stress in the peritubular capillary microenvironment mediates sepsis-induced renal microcirculatory failure and acute kidney injury. *Am J Pathol* 180:505–516.
Wu L, Gokden N, and Mayeux PR (2007a) Evidence for the role of reactive nitrogen species in polymicrobial sepsis-induced renal peritubular capillary dysfunction and tubular injury. *J Am Soc Nephrol* 18:1807–1815.
Wu L and Mayeux PR (2007) Effects of the inducible nitric-oxide synthase inhibitor L-N(6)-(1-iminoethyl)-lysine on microcirculation and reactive nitrogen species generation in the kidney following lipopolysaccharide administration in mice. *J Pharmacol Exp Ther* 320:1061–1067.
Wu L, Tiwari MM, Messer KJ, Holthoff JH, Gokden N, Brock RW, and Mayeux PR (2007b) Peritubular capillary dysfunction and renal tubular epithelial cell stress following lipopolysaccharide administration in mice. *Am J Physiol Renal Physiol* 292:F261–F268.
Yasuda H, Yuen PS, Hu X, Zhou H, and Star RA (2006) Simvastatin improves sepsis-induced mortality and acute kidney injury via renal vascular effects. *Kidney Int* 69: 1535–1542.
Yuen PS, Dunn SR, Miyaji T, Yasuda H, Sharma K, and Star RA (2004) A simplified method for HPLC determination of creatinine in mouse serum. *Am J Physiol Renal Physiol* 286:F1116–F1119.
Zarjou A and Agarwal A (2011) Sepsis and acute kidney injury. *J Am Soc Nephrol* 22: 999–1006.
Zeng Y, Adamson RH, Curry FR, and Tarbell JM (2014) Sphingosine-1-phosphate protects endothelial glycocalyx by inhibiting syndecan-1 shedding. *Am J Physiol Heart Circ Physiol* 306:H363–H372.
Zhang G, Yang L, Kim GS, Ryan K, Lu S, O'Donnell RK, Spokes K, Shapiro N, Aird WC, and Kluk MJ, et al. (2013) Critical role of sphingosine-1-phosphate receptor 2 (S1PR2) in acute vascular inflammation. *Blood* 122:443–455.
Zhu Q, Xia M, Wang Z, Li PL, and Li N (2011) A novel lipid natriuretic factor in the renal medulla: sphingosine-1-phosphate. *Am J Physiol Renal Physiol* 301: F35–F41.

Address correspondence to: Dr. Philip R. Mayeux, 4301 West Markham Street, #611, Little Rock, AR 72205. E-mail: prmayeux@uams.edu